Identification of the Potential Hits for Hindering Interaction of SARS-CoV-2 Main Protease (M^{pro}) from the Pool of Antiviral Phytochemicals utilizing Molecular Docking and Molecular Dynamics (MD) Simulations

Chirag N. Patel[1π], Dharmesh G. Jaiswal[1π], Siddhi P. Jani[1], Naman Mangukia[1,2], Robin M. Parmar[3] and Himanshu A. Pandya[1]*

[1]Department of Botany, Bioinformatics, and Climate Change Impacts Management, School of Sciences, Gujarat University, Ahmedabad, 380009, India.

[2]Bioinnovations, Mumbai, India.

[3]Department of Zoology, School of Sciences, Gujarat University, Ahmedabad, 380009, India.

Details of correspondence

Prof. (Dr.) Himanshu A. Pandya

Department of Botany, Bioinformatics, and Climate Change Impacts Management, School of Sciences, Gujarat University, Ahmedabad 380009, Gujarat, India.

Email: hapandya@gujaratuniversity.ac.in

Supplemental Files

Figures

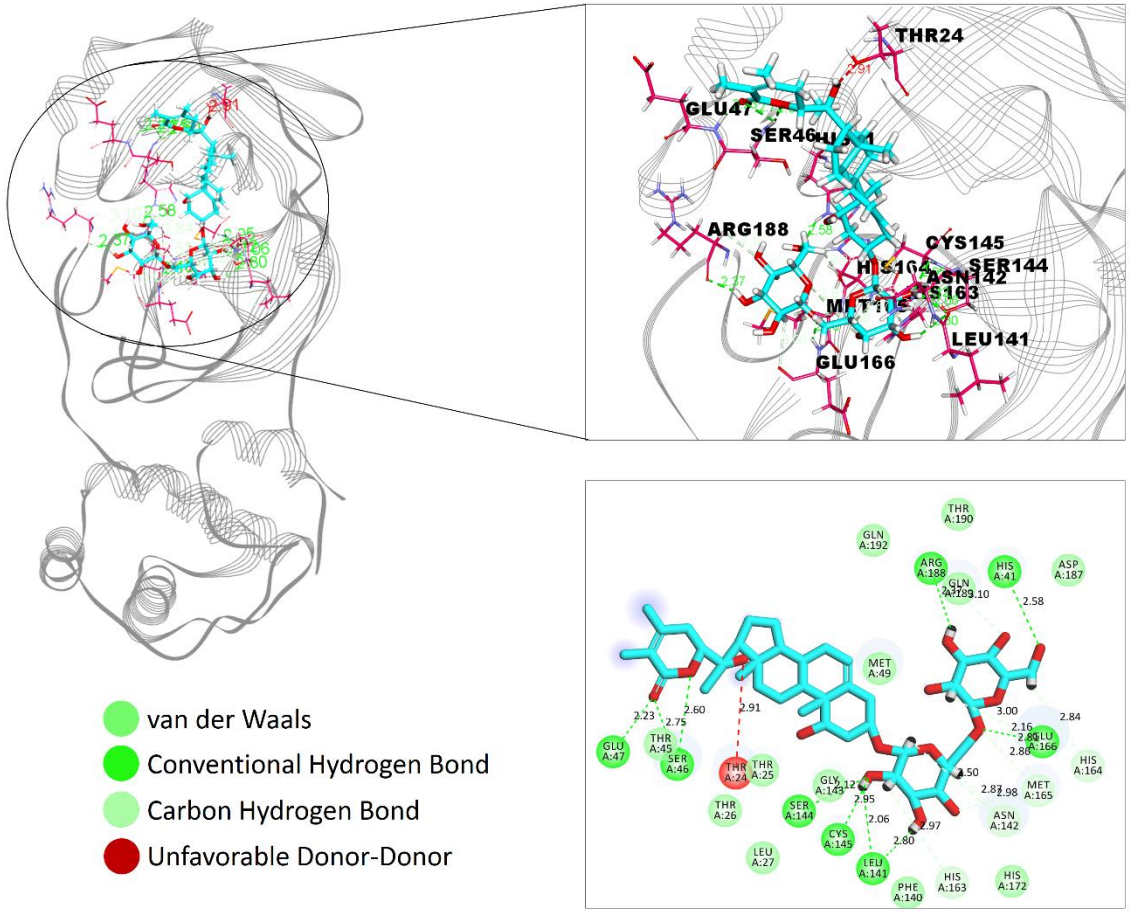

Fig-S1. Interaction of Withanoside VI in the binding cleft of SARS-CoV-2 M^{Pro} (PDB ID: 6LU7) of COVID-19 shown in (a) 3 D representation and (b) 2 D representation (for better clarity) describing ligands interactions by formation of various H-bonds and hydrophobic interactions with protein at the active site of the protein.

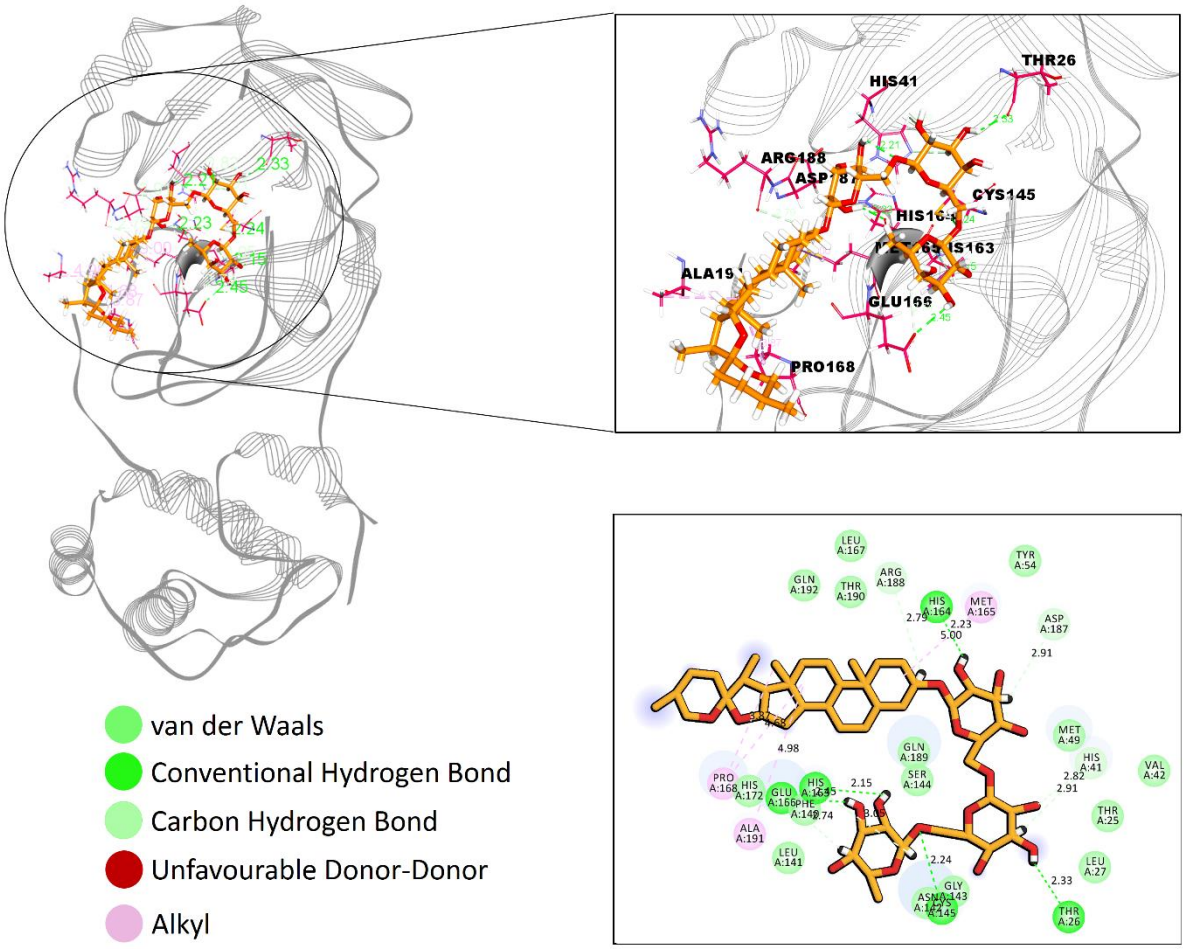

Fig-S2. Interaction of Racemoside B in the binding cleft of SARS-CoV-2 M^{Pro} (PDB ID: 6LU7) of COVID-19 shown in (a) 3 D representation and (b) 2 D representation (for better clarity) describing ligands interactions by formation of various H-bonds and hydrophobic interactions with protein at the active site of the protein.

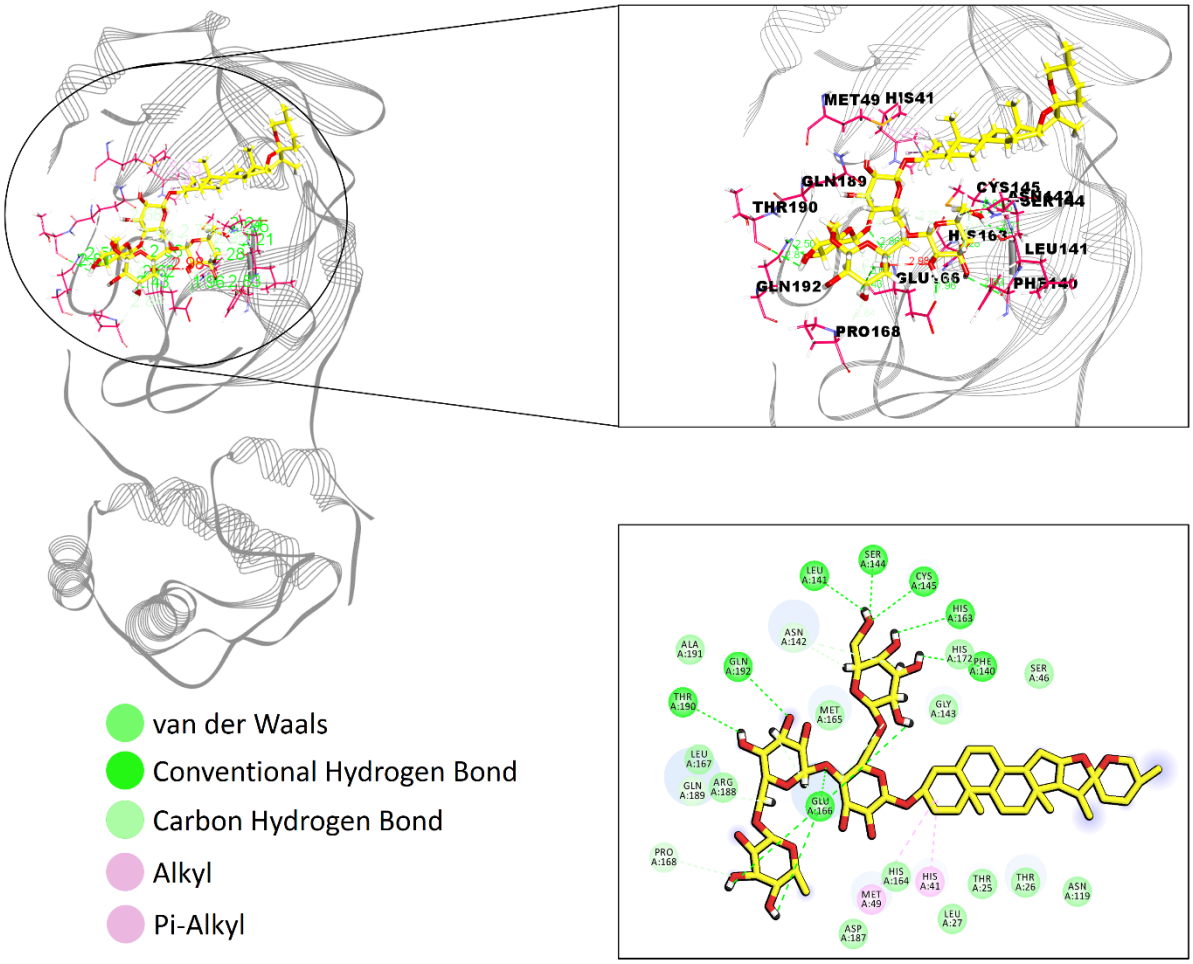

Fig-S3. Interaction of Racemoside A in the binding cleft of SARS-CoV-2 M^{Pro} (PDB ID: 6LU7) of COVID-19 shown in (a) 3 D representation and (b) 2 D representation (for better clarity) describing ligands interactions by formation of various H-bonds and hydrophobic interactions with protein at the active site of the protein.

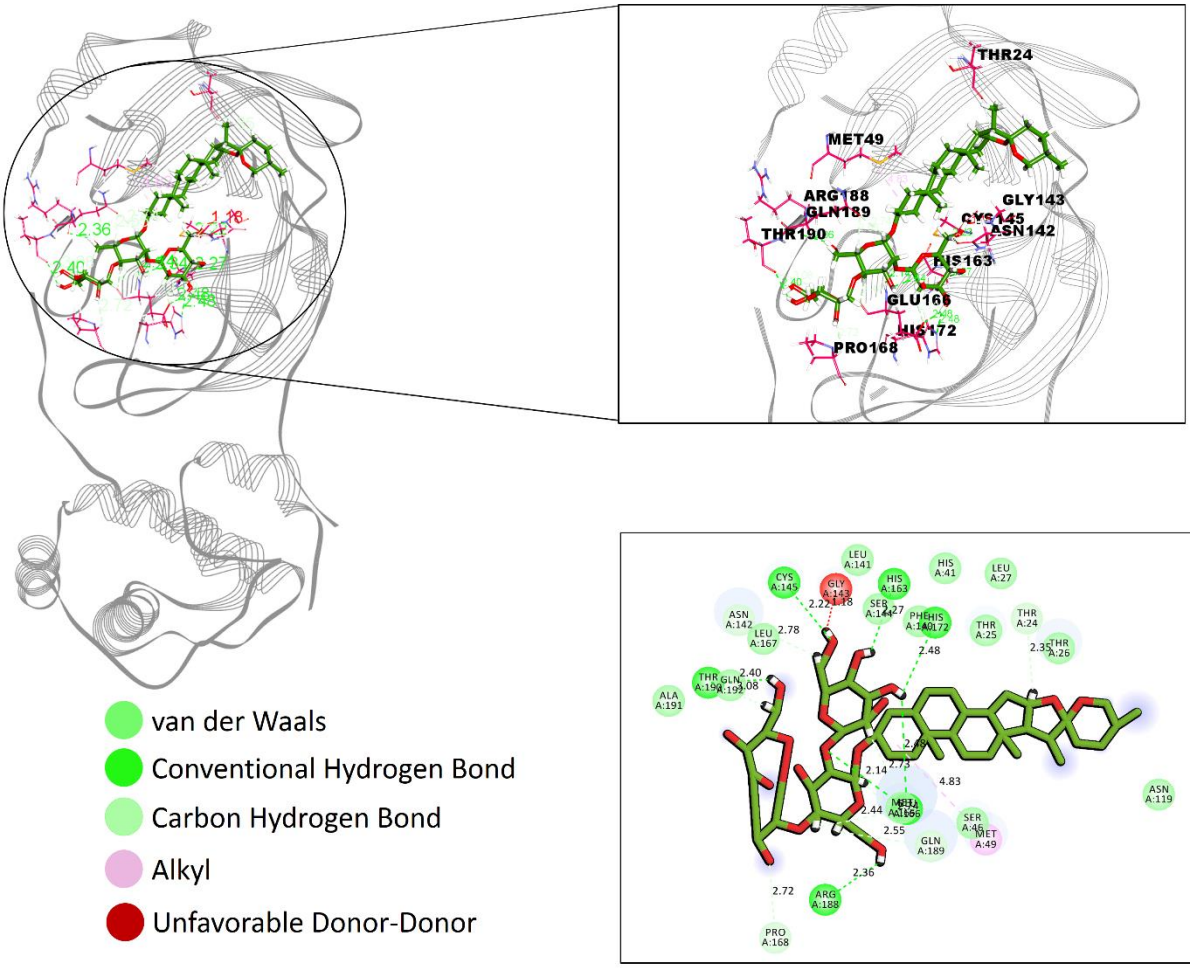

Fig-S4. Interaction of Shatavarin IX in the binding cleft of SARS-CoV-2 M^{Pro} (PDB ID: 6LU7) of COVID-19 shown in (a) 3 D representation and (b) 2 D representation (for better clarity) describing ligands interactions by formation of various H-bonds and hydrophobic interactions with protein at the active site of the protein.

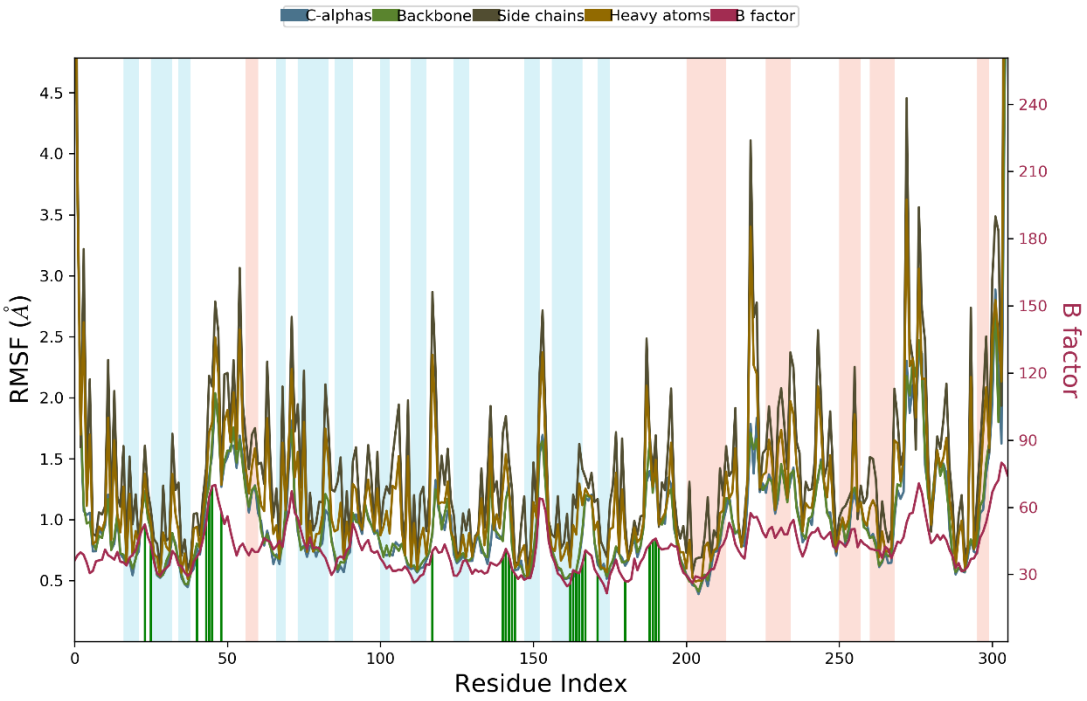

Fig-S5. RMSF plot of SARS-CoV-2 M^{Pro} target in complex with N3. The green bar plotted in the protein residue index corresponds to highly fluctuating amino acid residues.

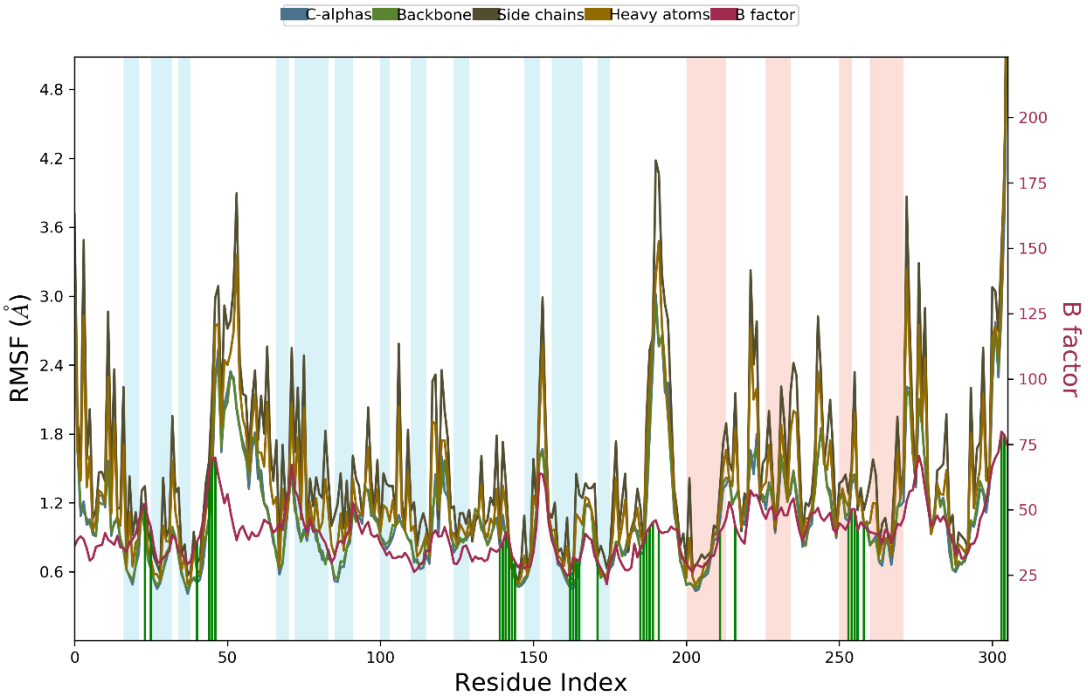

Fig-S6. RMSF plot of SARS-CoV-2 M^{Pro} target in complex with Withanoside V. The green bar plotted in the protein residue index corresponds to highly fluctuating amino acid residues.

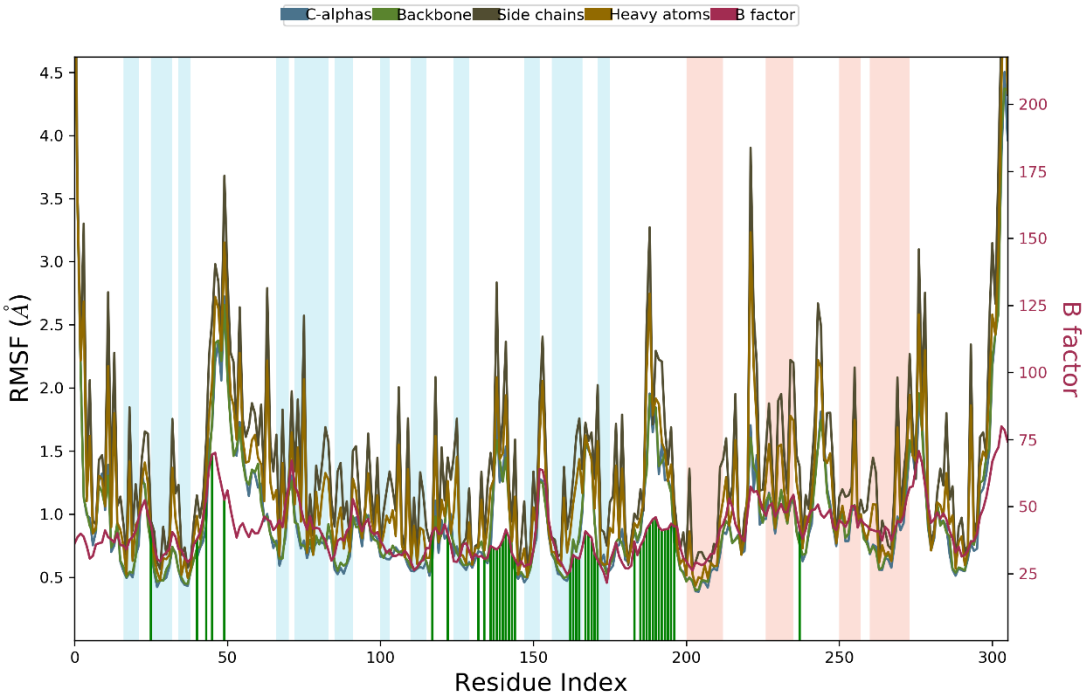

Fig-S7. RMSF plot of SARS-CoV-2 M^{Pro} target in complex with Withanoside VI. The green bar plotted in the protein residue index corresponds to highly fluctuating amino acid residues.

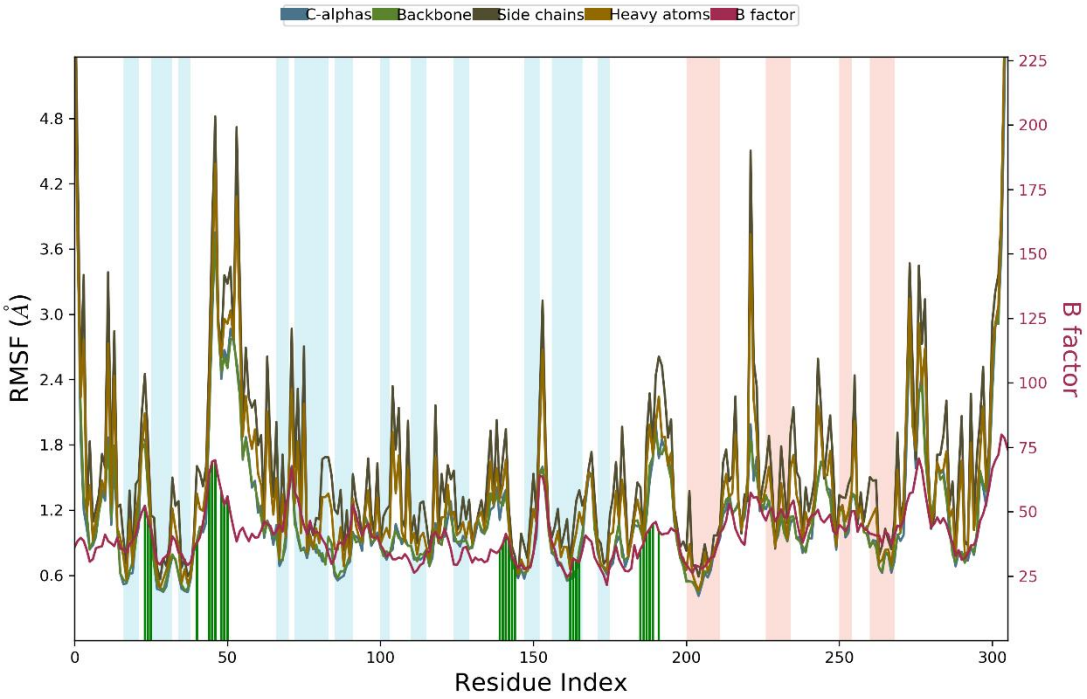

Fig-S8. RMSF plot of SARS-CoV-2 M^{Pro} target in complex with Racemoside B. The green bar plotted in the protein residue index corresponds to highly fluctuating amino acid residues.

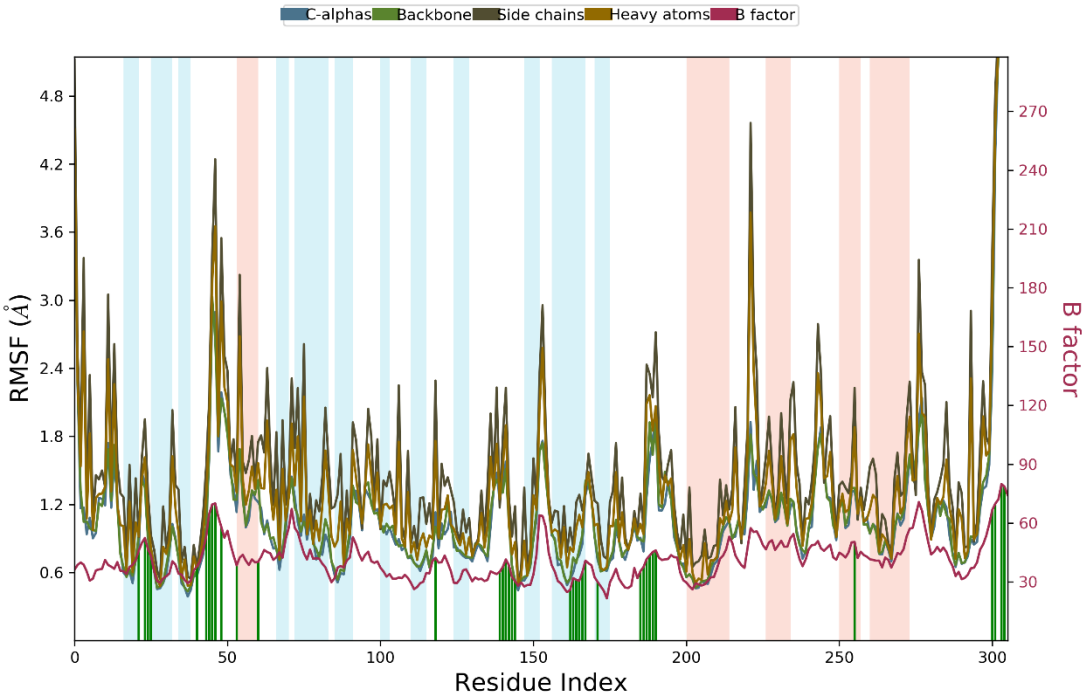

Fig-S9. RMSF plot of SARS-CoV-2 M^{Pro} target in complex with Racemoside A. The green bar plotted in the protein residue index corresponds to highly fluctuating amino acid residues.

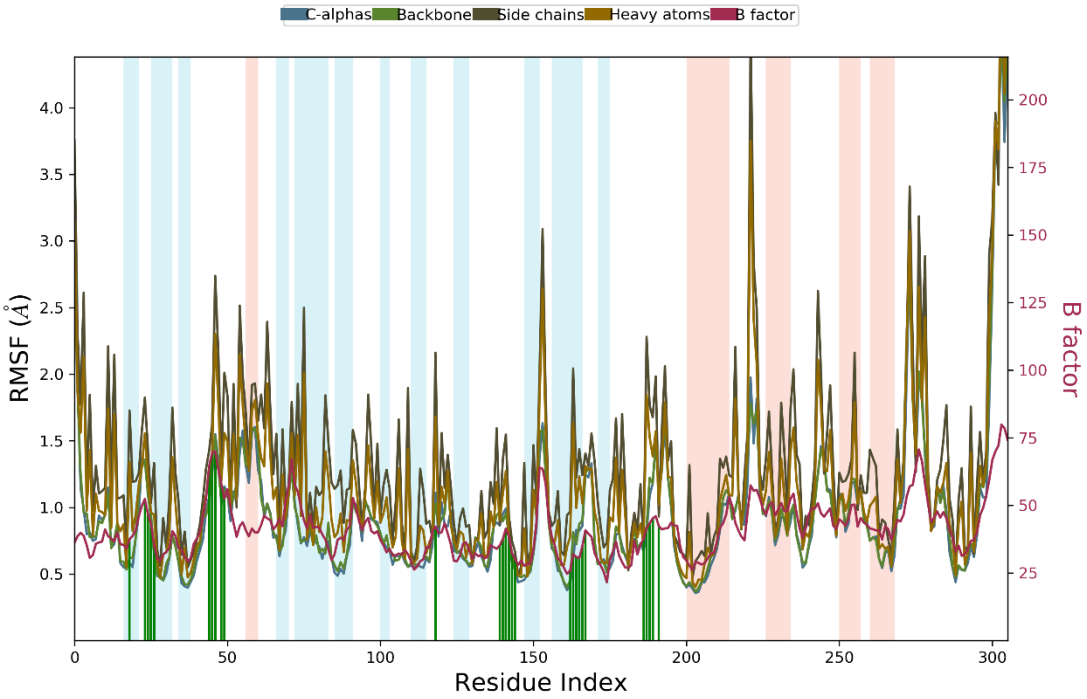

Fig-S10. RMSF plot of SARS-CoV-2 M^{Pro} target in complex with Shatavarin IX. The green bar plotted in the protein residue index corresponds to highly fluctuating amino acid residues.

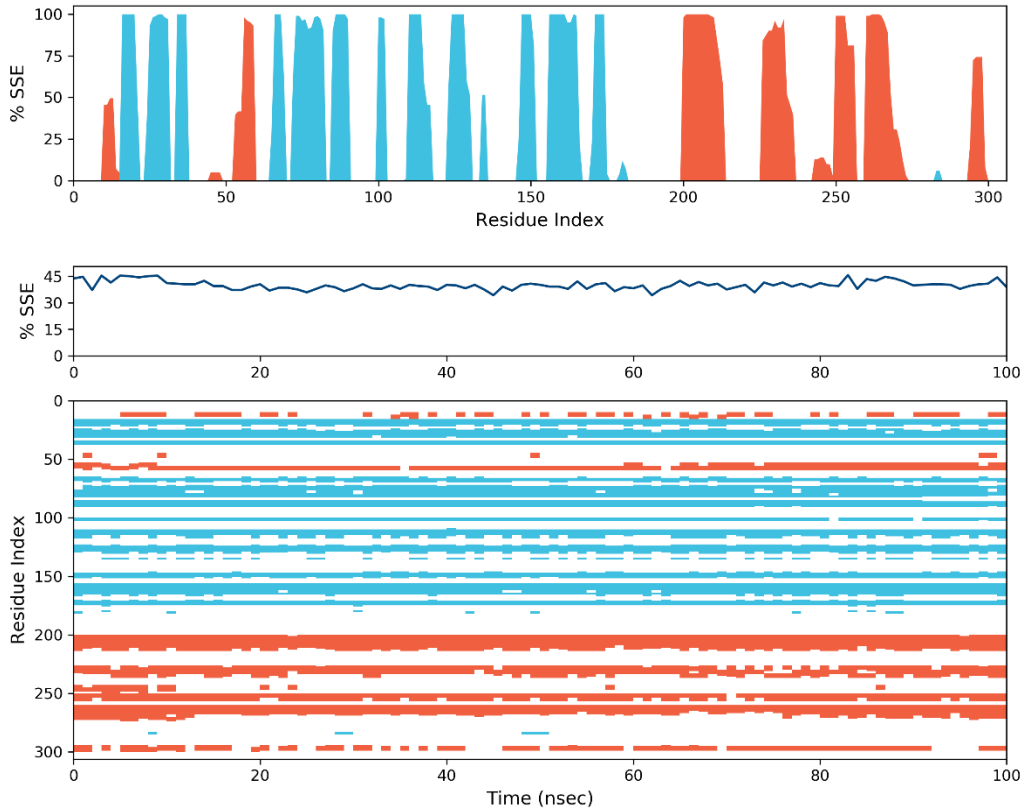

Fig-S11. The distribution of secondary structure elements of SARS-CoV-2 M^{Pro} target as a function of simulation time with co-crystal ligand, N3. The red and cyan colors represent helices and beta-sheets, respectively.

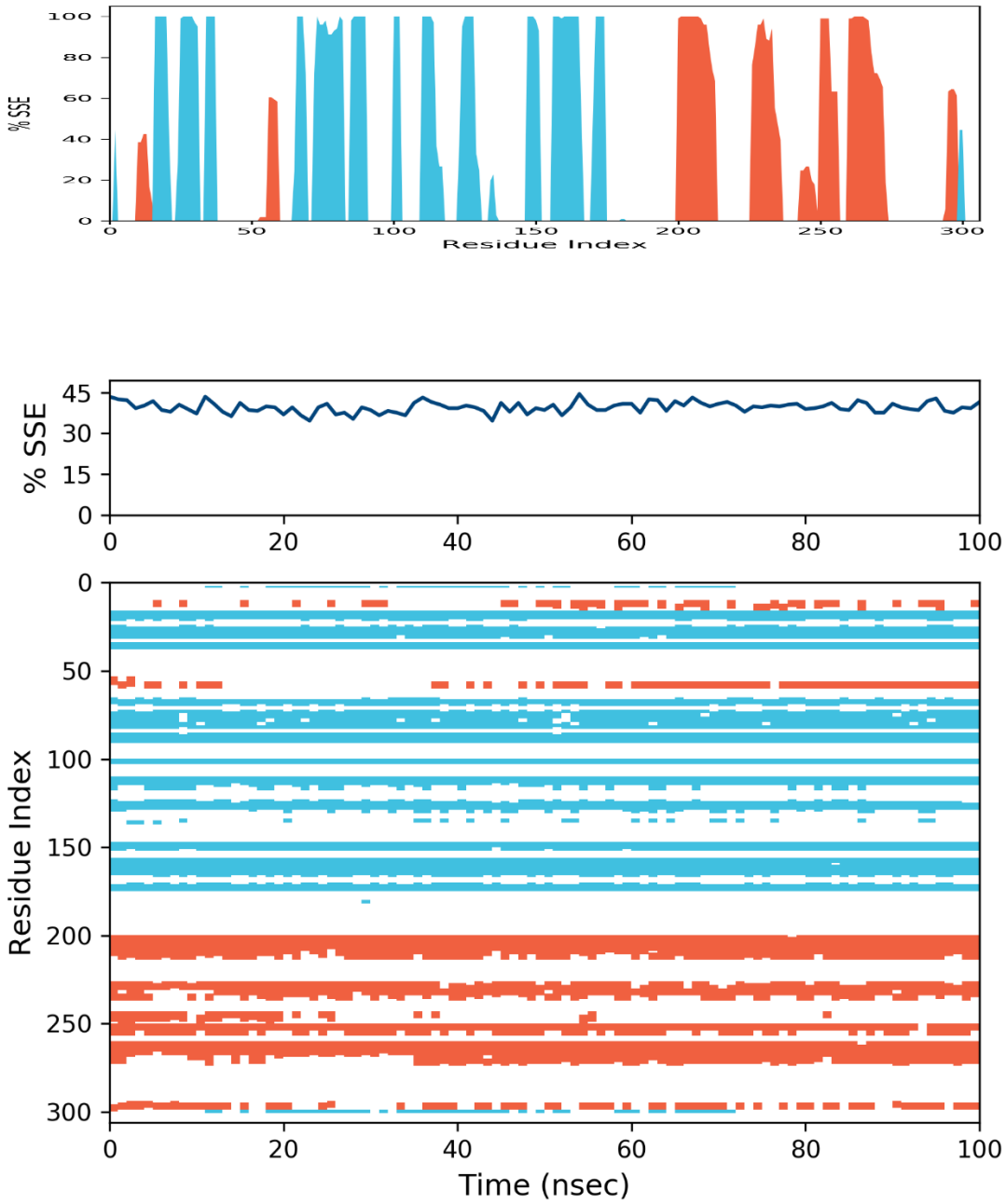

Fig-S12. The distribution of secondary structure elements of SARS-CoV-2 M^{Pro} target as a function of simulation time with Withanoside V. The red and cyan colors represent helices and beta-sheets, respectively.

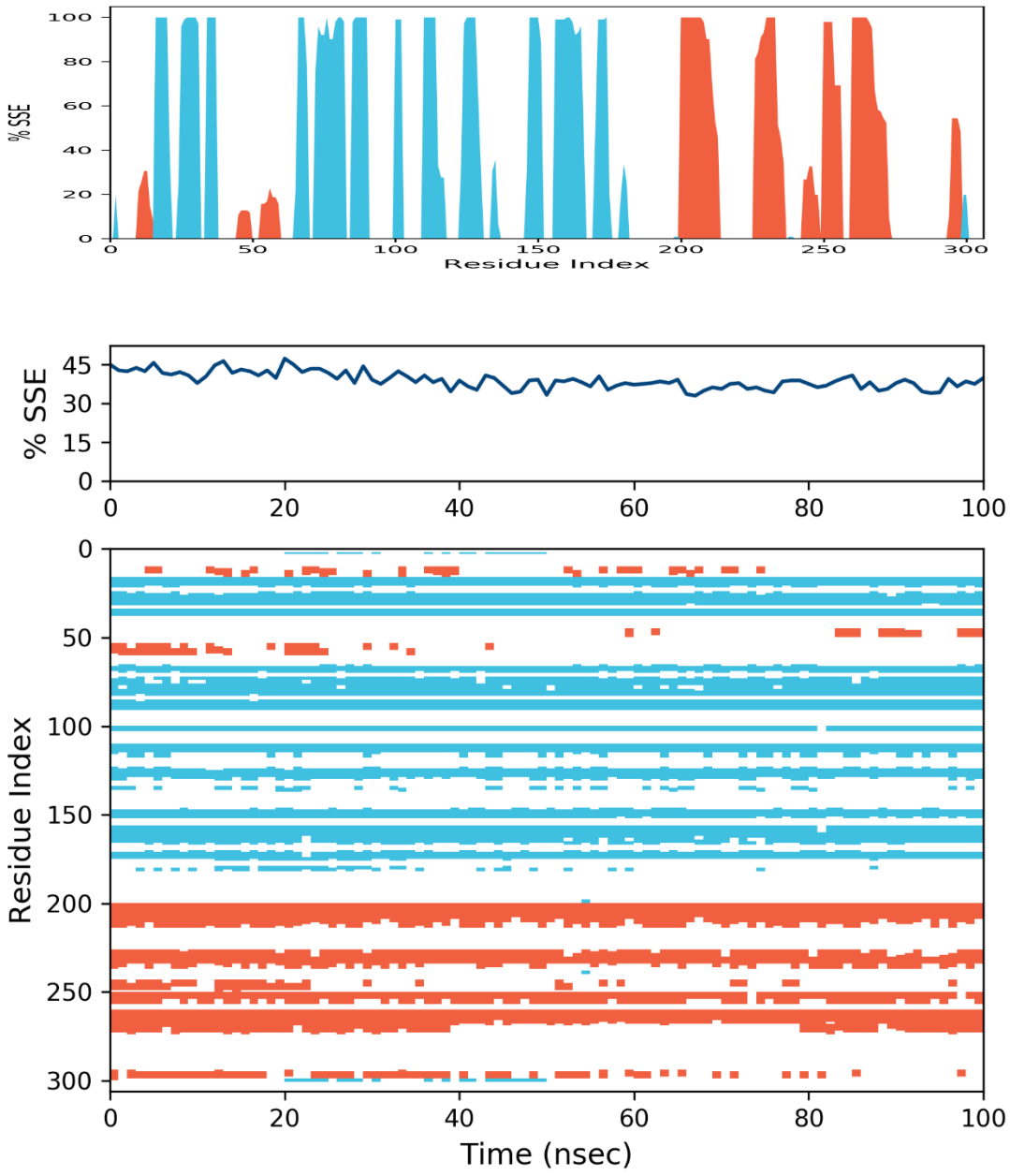

Fig-S13. The distribution of secondary structure elements of SARS-CoV-2 M^{Pro} target as a function of simulation time with Withanoside VI. The red and cyan colors represent helices and beta-sheets, respectively.

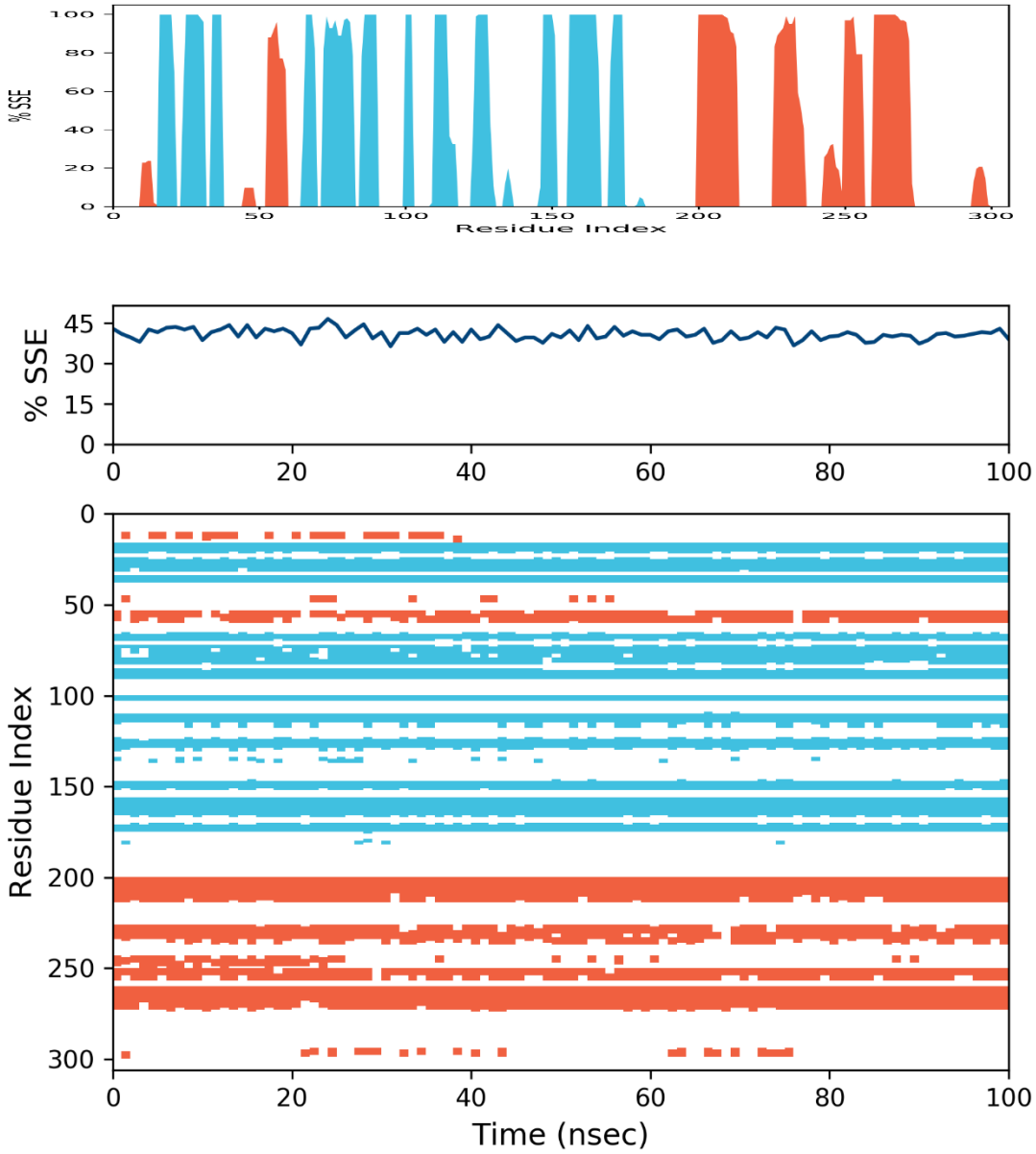

Fig-S14. The distribution of secondary structure elements of SARS-CoV-2 M^{Pro} target as a function of simulation time with Racemoside B. The red and cyan colors represent helices and beta-sheets, respectively.

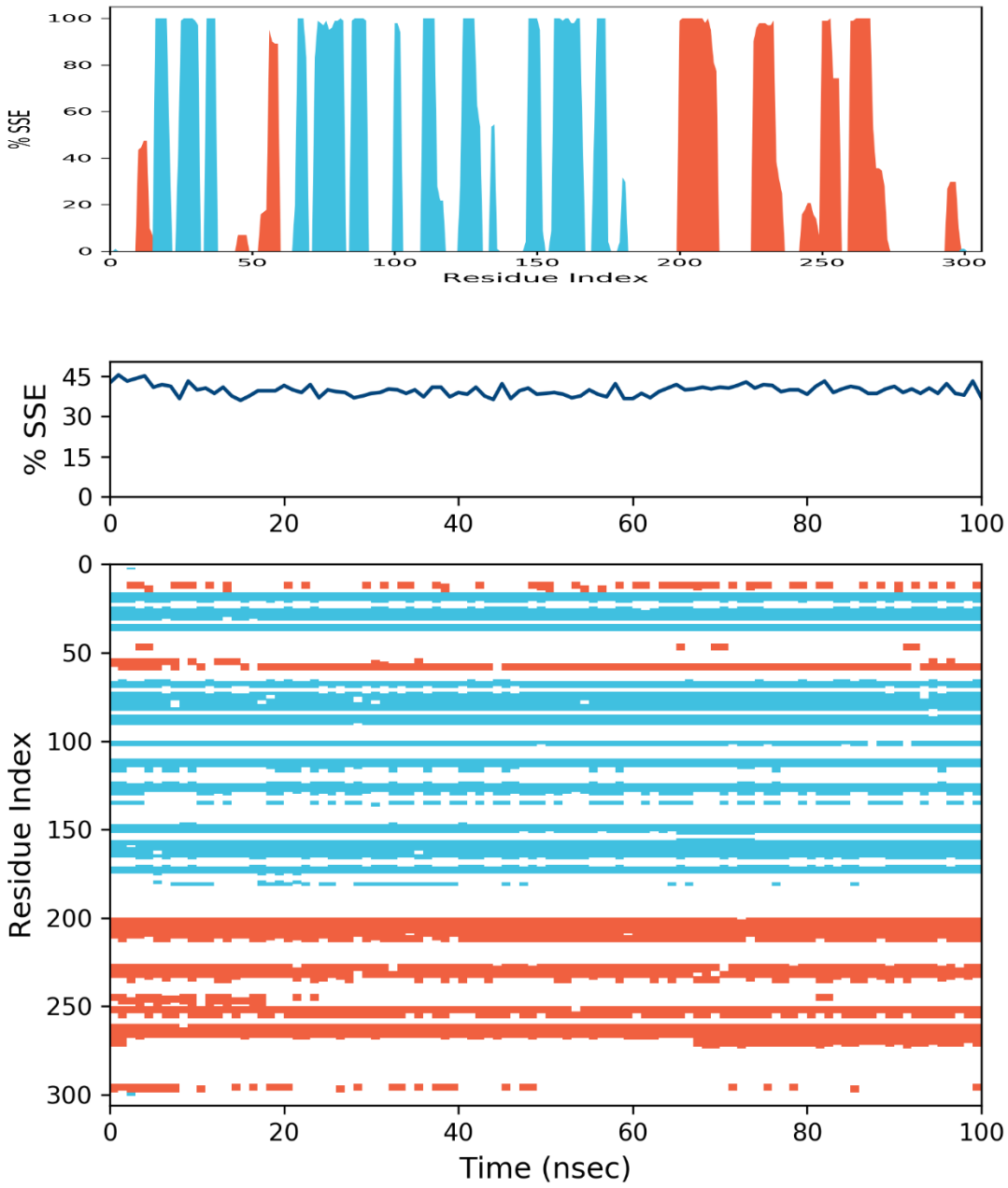

Fig-S15. The distribution of secondary structure elements of SARS-CoV-2 M^{Pro} target as a function of simulation time with Racemoside A. The red and cyan colors represent helices and beta-sheets, respectively.

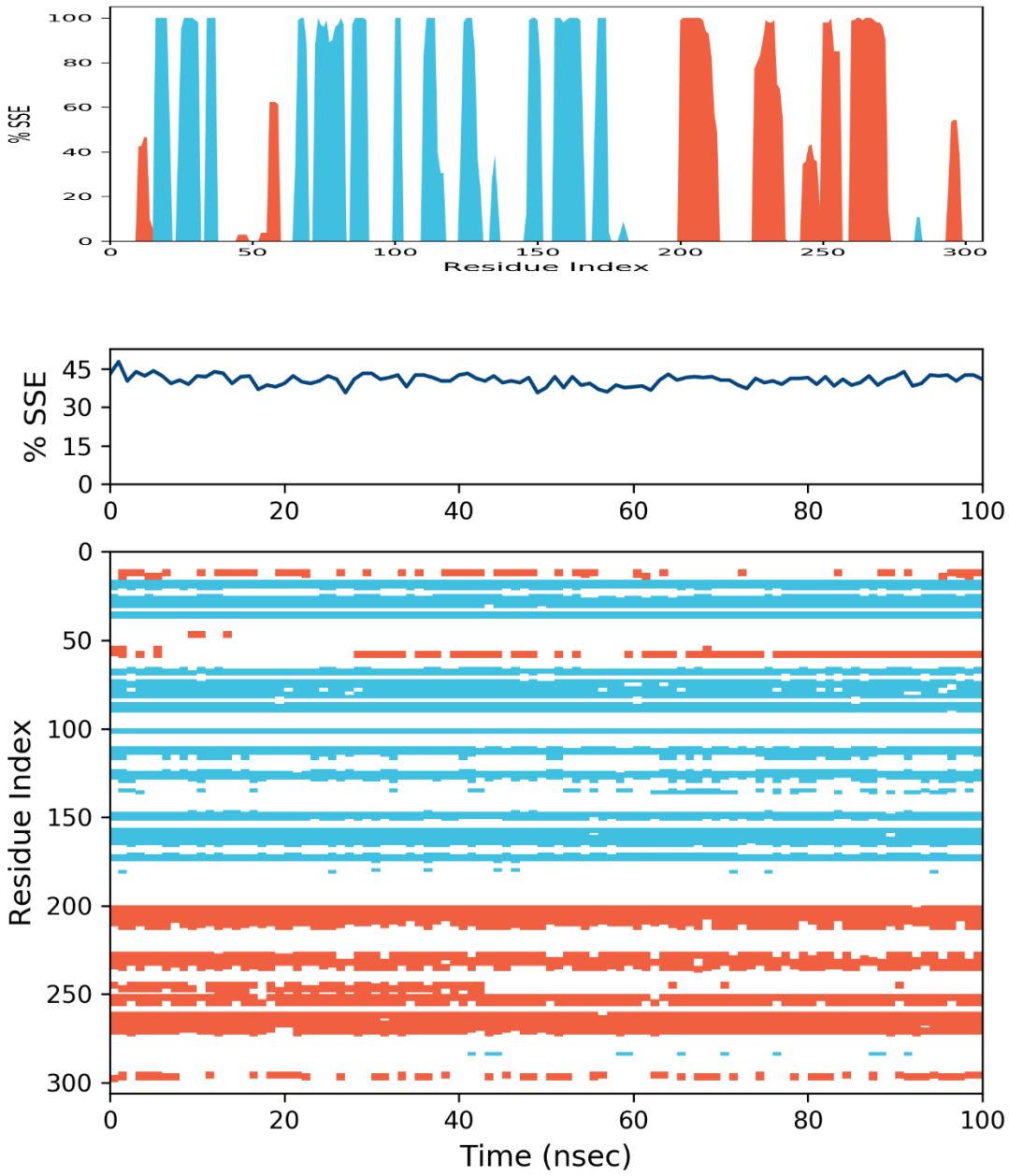

Fig-S16. The distribution of secondary structure elements of SARS-CoV-2 M^{Pro} target as a function of simulation time with Shatavarin IX. The red and cyan colors represent helices and beta-sheets, respectively.